

Changes in snow accumulation and ablation following the Las Conchas Forest Fire, New Mexico, USA

Adrian A. Harpold,^{1,2*} Joel A. Biederman,² Katherine Condon,² Manuel Merino,²
Yoganand Korgaonkar,³ Tongchao Nan,² Lindsey L. Sloat,⁴ Morgan Ross⁴ and Paul D. Brooks²

¹ University of Colorado, Institute of Arctic and Alpine Research, 1560 30th St Office 256, Boulder, Colorado 80303, USA

² University of Arizona, Hydrology and Water Resources, 1133 James Rogers Way Room 122 University of Arizona, Tucson, Arizona 85721, USA

³ University of Arizona, School of Natural Resources and the Environment, Tucson, Arizona, USA

⁴ University of Arizona, Ecology and Evolutionary Biology, Tucson, Arizona, USA

ABSTRACT

Seasonally, snow-covered forests are a critical source of water in the Western United States and are subject to major disturbances, including fire, harvest, disease and insect-caused mortality, that have relatively unknown effects on water availability. In this study, we investigated changes in winter season snow accumulation and ablation in a forest following the Las Conchas fire in the Jemez Mountains of New Mexico. We investigated two competing sets of processes that should determine the peak annual snowpack prior to snowmelt: (1) reduced interception by forest canopy results in greater new snow accumulation and (2) increased winter season ablation of the snowpack results in reduced peak snowpack volumes. These processes were evaluated with approximately 800 spatially distributed manual observations of new snow, 1500 manual observations of peak snowpack, and light detection and ranging-derived snow depth, vegetation and terrain datasets collected prior to the fire. A single snowfall event yielded significantly larger snow depths in the post-burn area versus the unburned area ($p < 0.001$), with 25% to 45% interception in the unburned area and near zero in the post-burn area. Conversely, the peak snowpack depths were significantly larger in the unburned area compared with the post-burn area (mean of 55 and 47 cm, respectively), despite nearly identical peak snowpacks prior to the fire (72 and 72 cm, respectively). The lack of strong vegetation controls led to less variability at peak snowpack in the post-burn area and a shift towards topographically controlled variability, caused by differences in elevation and aspect, occurring at larger spatial scales. The unburned area had roughly 10% more water available for melt than the post-burn area, with winter season ablation reducing snowpacks by nearly 50% prior to melt in the post-burn area. The relative importance of shortwave radiation to the snowpack energy balance and sublimation suggests that the 10% reductions in peak snow water storage found in these north-facing areas could be a conservative estimate for winter season ablation following fire. Further work is necessary to assess the role that topography plays in altering water partitioning following forest disturbance and the potential implications for ecological health and downstream water resources. Copyright © 2013 John Wiley & Sons, Ltd.



Supporting information may be found in the online version of this article.

KEY WORDS snow–vegetation interactions; forest fire; sublimation; snowpack energy balance; forest disturbance; water availability

Received 6 August 2012; Revised 10 December 2012; Accepted 10 December 2012

INTRODUCTION

Water resources in the Western United States are heavily reliant on snowmelt runoff from forested areas (Serreze *et al.*, 1999; Bales *et al.*, 2006) that are subject to a myriad of potential disturbances with relatively unknown effects on the larger-scale water balance (Barnett *et al.*, 2005; Adams *et al.*, 2011; Pugh and Gordon 2012). Prolonged droughts have directly resulted in forest die-off due to vegetative water stress (Breshears *et al.*, 2005; Breshears *et al.*, 2009) and indirectly exacerbated tree die-off from insects (Raffa *et al.*, 2008; Bentz *et al.*, 2010) and fire in the Western US forests (Marlon *et al.*,

2012). Forest fires have been increasing in size (Westerling *et al.*, 2006) and severity (Miller *et al.*, 2009) for the last several decades. In 2011 alone, an estimated of 8.7 million acres burned in the United States with an approximate cost of \$1 billion dollars (NOAA 2012). Drier and warmer than average conditions in the southwest in 2011 (NOAA 2012) contributed to the largest fires in New Mexico (Las Conchas Fire) and Arizona (Wallow Fire) state history. Removal of the forest canopy due to disturbance is likely to change the snowpack mass and energy budget in numerous and competing ways, but few observations exist (e.g. Burles and Boon, 2011) to corroborate initial model results (e.g. Seibert *et al.*, 2010; Pomeroy *et al.*, 2012). The increasing frequency and magnitude of fires highlight the need for a greater understanding of how large-scale fires affect snow processes and impact water availability for both society and the environment.

*Correspondence to: Adrian Adam Harpold, University of Colorado, Institute of Arctic and Alpine Research, 1560 30th St Office 256, Boulder, Colorado 80303, USA. E-mail: adrian.harpold@gmail.com

There are surprisingly few direct observations of snowpack processes following fire, and the existing evidence related to hydrological response following disturbance is mixed. Limited observations of earlier and larger snowmelt runoff in surface water following mountain pine beetle disturbance (Bethlahmy 1974; Potts 1984; Zhang and Wei 2012) and forest fire (Campbell and Morris, 1988) suggest that sub-canopy hydrological processes can be significantly affected by forest disturbance. It is generally accepted that removal of forest canopy, whether from tree death, fire or logging, will both increase snow accumulation by reducing interception (Haupt 1951; Kittredge 1953; Anderson 1956; Troendle and King 1987; Winkler *et al.*, 2010; Pugh and Small 2011) and increase winter season ablation (prior to peak snowpack and melt) from higher radiative and turbulent energy fluxes to the snowpack (Rinehart *et al.*, 2008; Veatch *et al.*, 2009; Gustafson *et al.*, 2010); Burles and Boon, 2011; Biederman *et al.*, in press), possibly causing a larger and more rapid snowmelt (Pugh and Gordon 2012; Winkler *et al.*, 2010; Seibert *et al.*, 2010; Burles and Boon, 2011; Zhang and Wei 2012; Pomeroy *et al.*, 2012). However, snowfall and streamflow response are highly variable (Bethlahmy 1974; Potts 1984; Bales *et al.*, 2006), and peak snow water equivalent (SWE) may not increase following widespread insect-induced tree die-off in the central Rocky Mountains (Biederman *et al.*, press). These observations draw attention to the lack of spatially distributed, detailed observations of the accumulation and ablation of snowpacks following forest disturbance. Most observations and modelling of the snowpack energy balance come from unforested and often relatively flat sites (e.g. Cline 1997; Marks and Dozier 1998), Burles and Boon, 2011), whereas most of the Western North America is a mosaic of forest structure and disturbance (Jost *et al.*, 2007) across complex topography (e.g. Ellis *et al.*, 2011). As changes in both climate and vegetation structure accelerate, water management decisions require better prediction of the cumulative impacts of forest disturbance on snowpack across topographically complex terrain.

The forest canopy alters the snowpack energy and mass balances at scales of individual trees to large watersheds. At the tree to plot scale, a healthy forest canopy will intercept and subsequently sublimate 25% to 45% of the incoming snowfall (Hedstrom and Pomeroy 1998; Pomeroy *et al.*, 1998) and emit longwave radiation (Pomeroy *et al.*, 2009; Lawler and Link 2011); these processes tend to reduce accumulation and increase ablation. At the stand to watershed scale, the forest canopy can minimize and delay ablation by reducing wind speeds and turbulence (Bergen 1971; Bernier 1990; Molotch *et al.*, 2009), shading the snowpack (Veatch *et al.*, 2009; Gustafson *et al.*, 2010) and decrease the albedo of the earth surface and alter the scattering of shortwave radiation (Rinehart *et al.*, 2008; Mahat and Tarboton 2012). The forest canopy can also create preferential scouring and deposition areas from wind re-distribution (Winstral and Marks 2002) and provide feedbacks to control the abundance and types of vegetation (Molotch *et al.*, 2011). Many of these snowpack–vegetation interactions are highly dependent on interactions between forest structure and

topography (i.e. elevation, slope and aspect), which means that it is often difficult to distribute detailed plot-scale observations to the larger areas where resource management decisions are made.

In this study, we make the first observations of stand and watershed-scale snowpack processes following the high-intensity Las Conchas fire in northern New Mexico, USA, to better understand how new snow accumulation and annual peak snowpacks were affected following fire. Specifically, we evaluate two sets of processes that have compensatory effects on net snow water input at peak snowpack in post-burned forests: (1) reduced interception by forest canopy results in greater new snow accumulation and (2) increased winter season ablation from the snowpack results in reduced peak snowpack volumes. To evaluate these processes, we use three data sets from paired burned and unburned forests: (1) spatially distributed manual observations of new snow fall; (2) spatially distributed manual observations of total snow depth and SWE at peak accumulation and (3) catchment-wide light detection and ranging (LiDAR) snow depth, vegetation and terrain observations obtained in the paired areas the year before the fire.

METHODOLOGY

Study site description

The Valles Caldera National Preserve is 30 km southwest of Los Alamos, NM, in the volcanic Jemez Mountains. The study site is located on Rabbit Mountain, near the southern boundary of the Valles Caldera National Preserve (Figure 1), which is part of the 22-km diameter Valles Caldera formed 1.13 Ma. Los Alamos, located approximately 10 km west and 1000 m lower than the field site, has a mean annual precipitation of 48 cm, of which 35% falls as snow between October and April, with annual temperatures averaging 9 °C from 1980 to 2011 (WRCC, accessed: 8/1/2012). Inter-annual variability in winter precipitation is high, coefficient of variation for October to April precipitation was 45% from 1980 to 2011 (Western Regional Climate Center (WRCC) 2012), but seasonal snowpacks generally develop on north-facing areas every year. Snowmelt and spring rains supply the majority of annual runoff due to hydrological connections between the upslope hillslopes and the stream network (Liu *et al.*, 2008). High evapotranspiration during the growing season reduces the influence of summer monsoon rainfall on runoff generation and water yield (Liu *et al.*, 2008).

An unburned and post-burn area were selected on Rabbit Mountain for intensive snow surveying (Figure 1) that had very similar topography and pre-burn vegetation (Figure 2). The vegetation above 2740 m was mixed-conifer spruce–fir forest dominated by Douglas fir (*Pseudotsuga menziesii*), white fir (*Abies concolor*) and blue spruce (*Picea ungens*), with interspersed stands of aspen (*Populus tremuloides*). Below 2740 m, at the toe-slope of the northern parts of Rabbit Mountain, were ponderosa pine (*Pinus ponderosa*) and Gambel oak scrubland (*Quercus gambelii*) communities.

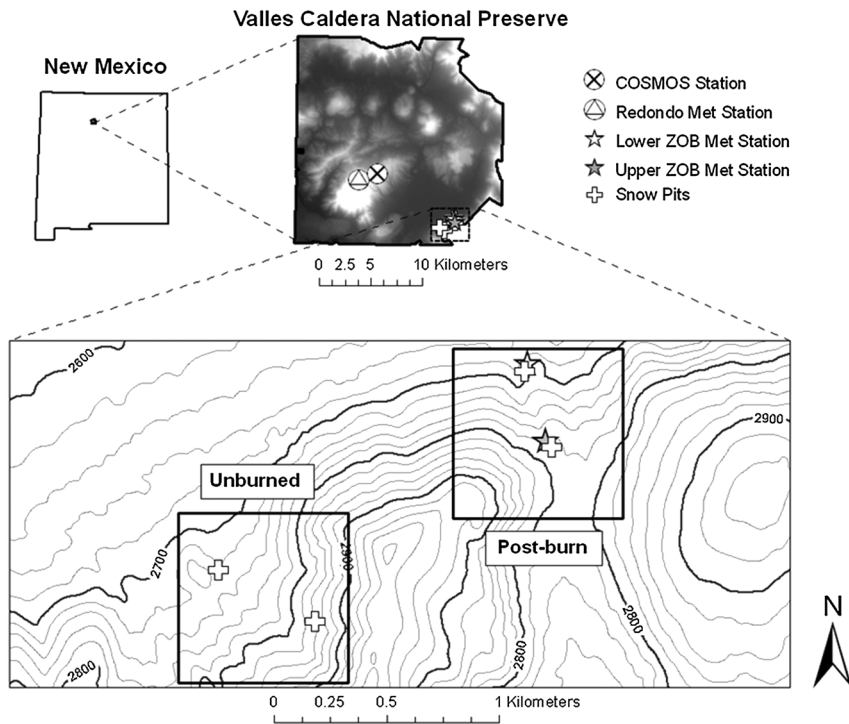


Figure 1. Overview of the study site showing the locations relative to New Mexico and Valles Caldera National Preserve. The hydrometeorological stations and snow pit locations are also shown. The boxes in the bottom panel correspond to Figure 2.

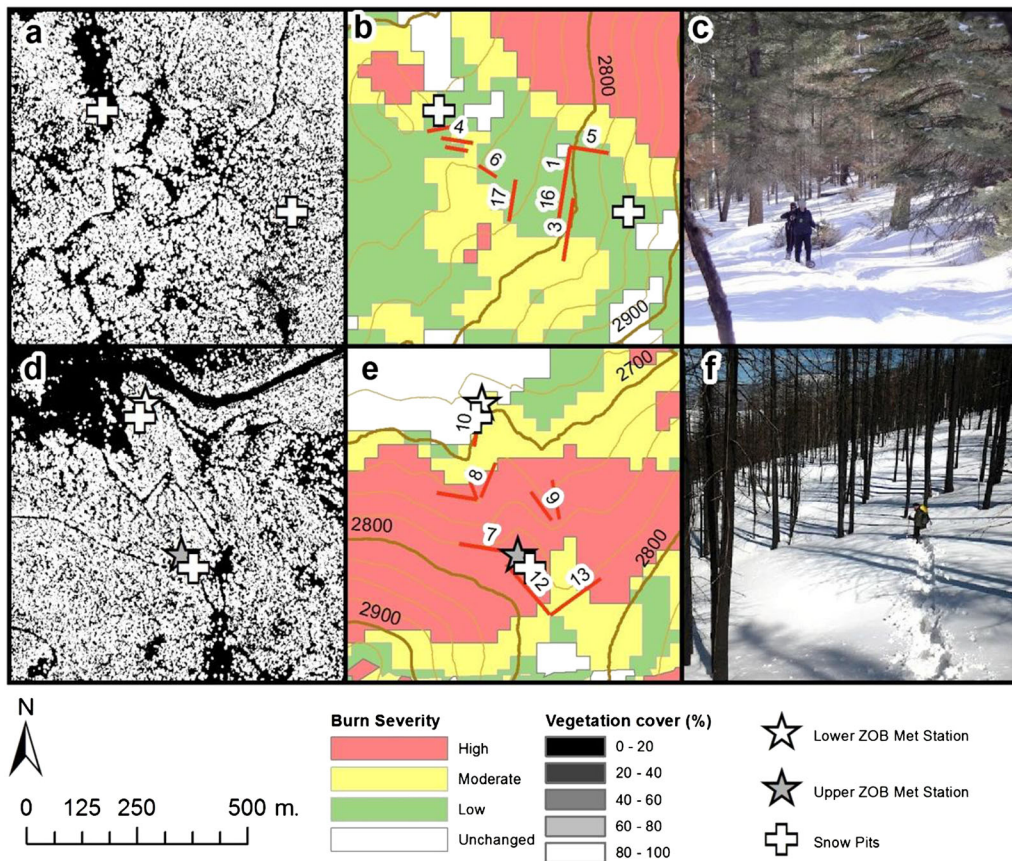


Figure 2. The canopy density, burn severity map and photographs for the 2012 snow survey. The LiDAR-derived canopy density collected prior to the fire in the 2010 unburned site (2a) and pre-burn site (2d). The burn severity estimates for the 2012 unburned site (2b) and post-burn site (2e). Photographs of peak accumulation in the 2012 unburned site (2c) and post-burn site (2f).

In 2010, prior to the fire, the pre-burn area had a similar forest canopy structure to the unburned site in terms of mean tree height (6.5 and 8.2 m, respectively), canopy density (57% and 71%, respectively), and the spacing and distribution of forest edges and canopy gaps (Figure 2a and d). The pre-burn and unburned sites were also similar topographically, with steep slopes (15° to 18° on average), a tight elevation range (2700 to 2800 m) and a predominantly north to northeastern aspect (Table I and Figures 1 and 2).

The Las Conchas fire was caused by a tree falling onto a power line on 26 June 2011 and ultimately burned 634 km² before it was 100% contained on 3 August 2011 (<http://www.inciweb.org/incident/2385/> accessed: 7/11/2012). The severity of the fire is illustrated by the burning of 174 km² in the first day, with an average rate of 12 ha per min (<http://www.inciweb.org/incident/2385/>). A crown fire burned much of Rabbit Mountain with high burn severity in all but a few areas (<http://www.inciweb.org/incident/2385/>), which left dead and branchless trees (10 to 30 m) during the 2012 winter season. The fire on Rabbit Mountain was at a sufficient temperature to combust the organic soils, many of which were subsequently eroded by the 2011 monsoon rains. In November 2011, several small catchments on Rabbit Mountain were heavily instrumented to study the effects of fire on the coupled water, carbon and energy cycle (Figure 1) as part of the Jemez River Basin Critical Zone Observatory (www.czo.arizona.edu).

Winter season hydrometeorological datasets

We focus on winter season data from 2012 following the Las Conchas fire; however, 2010 data are also introduced to show similarity between the areas prior to the fire. The meteorological measurements were made approximately 10 km away at 3230 m in an open site on the Redondo Massif (Figure 1) in 2010 and 2012 (Table II) and in the post-burn area on Rabbit Mountain in 2012 (Figures 1 and 4). Winter season meteorological measurements were averaged from November 1 to March 15 (Table II), with the exception of winter precipitation, which was measured with a shielded tipping bucket holding anti-freeze from November 1 to the day of the peak snowpack survey in that year. Two additional micro-meteorological stations were installed in November 2011 in the post-burn area at elevations of 2680 and 2780 m

Table I. Topographic properties (elevation, slope and aspect) and pre-fire vegetation properties (tree height and canopy density) for the two field sites.

	Unburned 2012	Post-burn 2012
Elevation (m)	2777 (2720–2832)	2749 (2692–2792)
Slope (%)	15.3 ± 5.2	17.8 ± 7.2
Aspect (degrees CW from S)	262 ± 82	200 ± 140
	Unburned 2010	Pre-burn 2010
Tree height (m)	6.5 ± 6.3	8.2 ± 6.2
Canopy density (%)	57 ± 42	71 ± 39

The data is shown as the mean ± one standard deviation, with the exception of elevation, where the range of data is shown in parentheses.

Table II. Hydrometeorological data for the winter season (11/1 to 3/10) of 2010 and 2012.

	2010	2012
Ta (°C)	−5.5	−4.7
% RH	65	61
Wind speed (m/s)	1.49	1.64
R _{net} (W/m ²)	267	250
Precipitation (m)	0.336	0.209
Max SWE (m)	0.328	0.191
Length of winter season (days)	179	161

The mean air temperature (Ta), relative humidity (RH), net radiation (R_{net}) and precipitation were collected at the Redondo meteorological station. The maximum snow water equivalent (SWE), length of snow season and date of maximum SWE were collected at the Quemazon SNOTEL station, except for the 2012 length of season, which was estimated on the basis of snow depth sensors in the post-burn area.

(Figure 2). Time series for air temperature, relative humidity, wind speed and net radiation (Figure 3) are shown and discussed with regard to potential ablation processes during the 2012 snow season. Snow depth measurements and snow season length were estimated for 2010 and 2012 from the

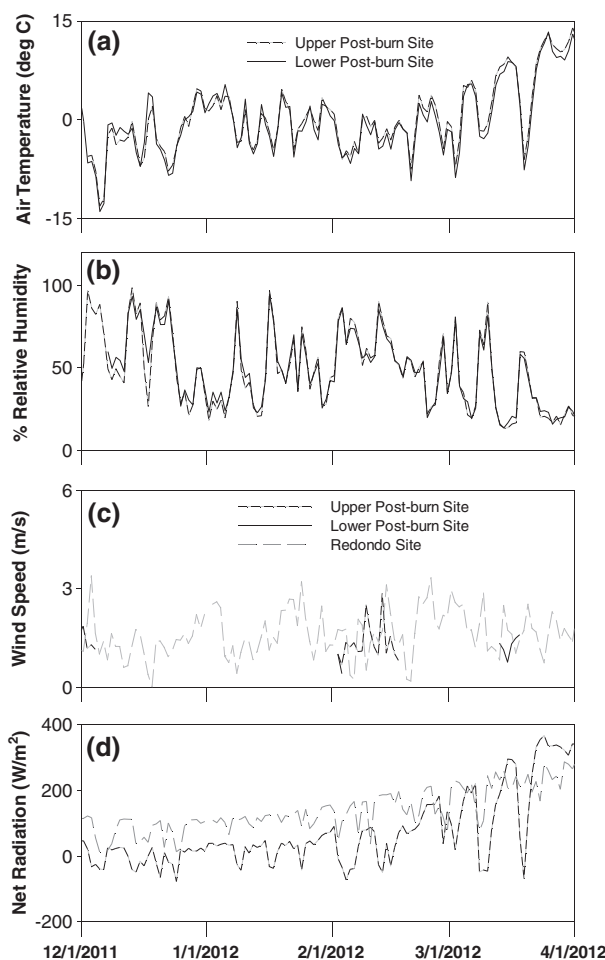


Figure 3. Time series of meteorological data during the 2012 snow season at the post-burn site (Figure 2). Temperature and relative humidity were measured at two locations (3a and 3b, respectively). Wind speed data is lacking in the post-burn site and additional data from Redondo is shown (Figure 3c). Net radiation is measured only at the upper site (3d).

Quemazon SNOTEL station, located about 5 km to the east, to compare our measurements to a standardized snow product. Two continuous snow depth sensors in the post-burn area showed similar timing and magnitude of snow accumulation to the Quemazon SNOTEL station in 2012.

Snow survey design

Snow surveys were collected on 10/3/2012 to 12/3/2012 over approximately 50 ha that represented multiple slopes and aspects of both burned and unburned forested catchments. Survey transects were 50 to 150 m in length and along cardinal magnetic directions (Figure 2b and e). Depth measurements were made at 5-m centres, as well as 1 m to the front, back, left and right, and the means of the resulting 5-point 'diamond' were used for statistical comparisons. New snow observations were made following a single storm that occurred on 9/3/2012 and 10/3/2012, which was then subtracted from the total snow depth to estimate the peak snowpacks on 9/3/2012. Peak snowpacks were defined in this way to reduce the correlation between new and peak snow depths and provide a better estimate of integrated winter season effects on snow processes prior to maximum accumulation. An observation of overhead canopy density was made at each 5-m centre point using the categories open, sparse, medium and dense. Transects were selected to characterize the unburned area and post-burn area (Figures 1 and 2) based on aerial burn severity maps (Figure 2b and e) and visual observation (Figure 2c and f). In total, over 1500 peak snow depth observations and almost 500 new snow depth observations were made.

Four snow pits, with two each in the unburned and post-burn areas, were installed at roughly 2700 and 2800 m elevation. Fewer snow density measurements were required than snow depths because density typically exhibits much lower spatial variability than depth (Elder *et al.*, 1998). Each pit was excavated to the soil surface and snow density, grain type and size, and temperature were measured at 10-cm vertical increments. The 10-cm observations of snow density were integrated to obtain an average snowpack density and multiplied by depth to obtain SWE. SWE values were normalized by observations of winter season precipitation (from November 1 to date of snow survey) from nearby meteorological stations to obtain SWE:*p* ratios, which indicated the fraction of snowfall remaining in the snowpack at peak accumulation.

Spatial datasets

Several spatial datasets were used to identify burn severity, determine local topography and estimate peak snow depths and vegetation characteristics prior to the Las Conchas Fire. The burn severity map was developed using aerial photography and some ground-truthing (USDA, 2011) and was used to identify potential snow survey locations. A terrain model was developed at 1-m resolution for the locations of each snow survey observation using a LiDAR elevation dataset collected by the National Center for Airborne Laser Mapping (NCALM) in 2010. Vegetation height was estimated on the basis of the maximum LiDAR

return heights to within an accuracy of around 10 cm (NCALM, 2010). Vegetation density was estimated at each survey observation as one minus the fraction of first-return LiDAR pulses that reached the ground surface. Distributed snow depth measurements for 2010 were estimated by differencing a LiDAR dataset from peak snowpacks (1 April 2010) from a 'snow-off' LiDAR dataset. A mask was applied to remove from analysis areas where no LiDAR returns reached the snow surface or where the snow-off ground surface varied by more than 30 cm within a single 1 m² grid cell. The dense forests prior to the fire resulted in a reduction to roughly 750 LiDAR-derived snow depth data points from 2010 that were co-located with observations from 2012.

Statistical analysis

Several statistical tests were applied using Matlab (MathWorks Inc., Version 7.11.0 R2010b) to compare differences in snowpacks between burned and unburned areas and to determine how snowpacks were related to vegetation and topography before and after fire. Lilliefors tests (Sheskin 2004) were first applied to check the normality of the new and peak snow depth datasets using the four areas (unburned in 2010 and 2012, pre-burn and post-burn). *p*-values for the ToLilliefors tests were computed using inverse interpolation into a table of critical values in Matlab. New and peak snow depths were normally distributed in all areas ($p < 0.05$), with the exception of the 2012 post-burn; thus, parametric statistical tests were assumed valid throughout. These four datasets were compared with one-way analysis of variance (ANOVA) (Sheskin 2004), which returns the *F*-statistic (the ratio of sum of squares to the degrees of freedom) and a *p*-value that is derived from the cumulative distribution of *F* (Mathworks, 2012). A grouped ANOVA (Sheskin, 2004) was performed for canopy density (open, sparse, medium and dense) and aspect categories (north, south, east, west), with the aforementioned four datasets, to test whether the mean values were different. If significant differences ($p < 0.05$) were observed, multiple one-way ANOVA were performed between all categories, to identify categories that were statistically different from one another. Linear correlations were also performed between the elevation and northness (where due north is unity and due south is zero) and peak snowpacks, and reported values include Pearson correlation coefficient and *p*-values (estimated using a Student *t*-distribution for a transformation on the correlation).

Patterns of spatial correlation were studied within each study area using experimental and modelled semivariograms. The experimental semivariogram

$$\gamma = \frac{1}{2N(h)} \sum_{i=1}^{N(h)} [z(x_i) - z(x_i + h)]^2 \quad (1)$$

is half the average squared difference in depth observation pairs *z* at locations *x*, separated by a lag distance *h*. *N*(*h*) is the number of such depth observations pairs in the given dataset. Semivariograms were calculated using the depth observations falling along the centreline of each survey (e.g. positions of

0, 1, 2, 5, 6, 7, ..., 99, 100, 101 m). Experimental semivariograms were fitted with exponential models to allow calculation of the sill, or variance approached at large lag distances, and the range, calculated as the lag distance at which the model semivariogram reaches 95% of the sill variance. Observations closer to one another than the range are autocorrelated, whereas those farther apart than the range are independent.

RESULTS

Maximum SWE in 2012 was approximately 82% of the historical average (1971 to 2000) at Quemazon SNOTEL station, whereas 2010 had 131% of the historical average, but the date of maximum SWE and length of the snow season were similar between years (Figure 4). Other than precipitation, winter meteorological forcings were similar in 2010 and 2012 (Table II), including average air temperature, relative humidity, wind speed and net radiation. There were minimal differences in air temperature, relative humidity and wind speed between the post-burn upper and lower meteorological stations in 2012 (Figure 3), consistent with the less than 100 m in elevation between the stations. The limited record of wind speeds at the post-burn area showed very similar wind speeds to those measured at a height of 3 m at the Redondo meteorological station (Figure 1), which averaged 1.64 m/s and never exceeded 6 m/s (hourly means) over the 2012 winter season (Figure 3c). Maximum snow depths in 2012 occurred on March 11 at the post-burn area, slightly later than at the lower elevation Quemazon SNOTEL, which showed a small decrease in SWE prior to the new snow accumulation on 9/3/2012 and 10/3/2012 (Figure 4).

The two snow pits from the unburned area had deeper snow and more SWE than those in the post-burn area in 2012 (Figure 5). Mean snow density was similar in both post-burn and unburned areas, with upper elevation snowpacks exhibiting slightly higher density than lower

elevations (approximately 26 kg/m^3 and 22 kg/m^3 , respectively). The crystal structure and layering was quite different between the unburned and post-burn areas (Figure 5). The post-burn area pits were entirely large facets with approximately 10 cm of new snow on the snow surface (Figure 5a and c). In contrast, the unburned area had large facets only in the bottom 15 cm of the snow profile, with a 20- to 30-cm layer of small facets, and a 20-cm layer of rounds making up the majority of the snowpack (Figure 5b and d). Ice layers were present in all the snow pits in 2012, and substantial densification events occurred at the snow depth sensors during late February and early March 2012 (Figure 4), suggesting that there were one or two small winter season surface melt events that re-froze in the snowpack.

New snowfall

The post-burn area received an average of 15 cm of new snowfall on 9/3/2012 and 10/3/2012, which is approximately 100% of the total input for that single event (as observed at the open-area continuous snow depth sensors shown in Figure 4). In contrast, only 12 cm of new snowfall reached the snowpack at open locations in the unburned area, indicating that total new snow inputs may have been 3 cm smaller in the unburned area. The mean of all new snow measurements was 9 cm in the unburned area, which suggests 25% to 45% of the new snow was lost to interception (depending on the total input estimate). As a result of the greater interception of new snowfall in the unburned area, the post-burn site had significantly larger new snowfall depths ($p < 0.001$) than the unburned area.

The new snowfall variability in the post-burn area had no relationship with forest structure, whereas the unburned area had significantly less new snowfall under dense canopy than in open canopy. The variances of the new snowfall depths in the two areas were both about 3 cm (Table III), but the unburned area had a coefficient of variation of 59% compared with just 35% in the post-burn area, because of the smaller mean in the unburned area. In the post-burn area, there were no statistical differences among new snowfall depths from different canopy categories (Figure 6b). In contrast, the unburned area had the smallest new snowfall depths under dense canopy and statistically significant differences ($p < 0.05$) between open and dense locations (Figure 6a).

Peak snowpack

Consistent with the observation of new snowfall, snowpacks were less spatially variable in burned areas versus unburned areas (Figure 7) at peak snowpack (defined as the snowpack prior to the storm on 9/3/2012). Clear differences were present in the snow depths and their relationships with vegetation densities along several example transects for the unburned (Figure 7) and post-burn area (Figure 7). In the unburned area, the peak snow depths varied from 0 to 88 cm (Figure 7) with a standard deviation of 17 cm (Table III), with lower depths under dense canopy and more snow in canopy gaps (Figure 7).

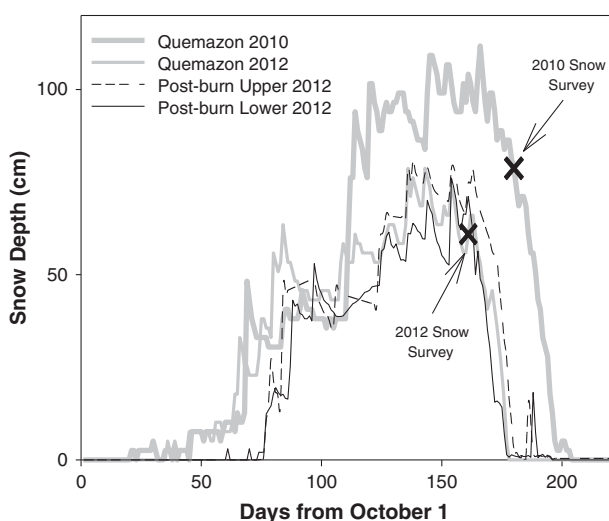


Figure 4. Comparison of snow depths from 2010 to 2012 at the Quemazon SNOTEL and from 2012 at the post-burn upper and lower sites (Figure 1). The dates of the snow surveys are noted.

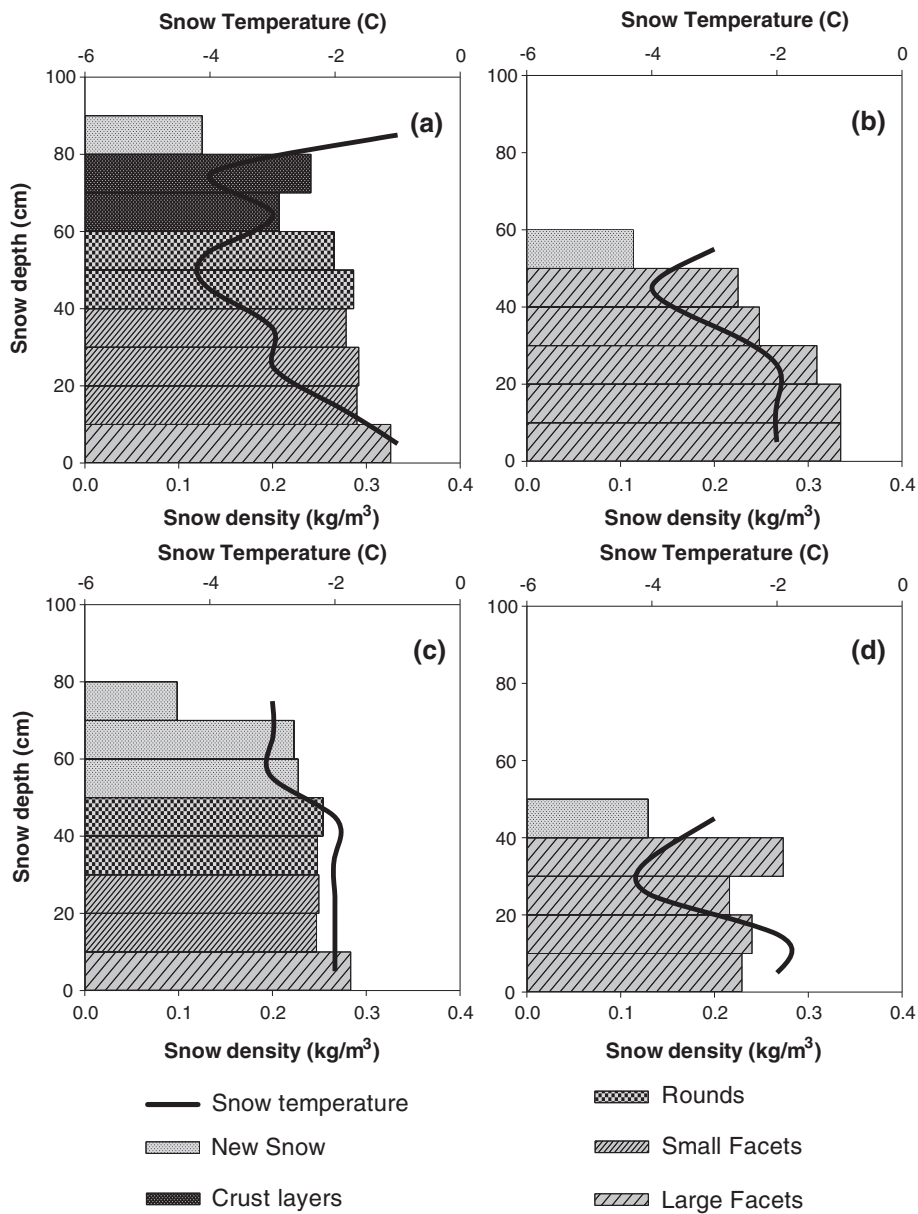


Figure 5. Observations of snow depth, structure, temperature and water equivalent (SWE) from upper and lower sites in the 2012 unburned site (5a and 5c, respectively) and 2012 post-burn site (5b and 5d, respectively). Density is shown on the primary (lower) axis corresponding to the bar lengths, and snowpack temperature is shown on the secondary (upper) and represented by a curved line. The shading of the bars represents the snow crystal structure described in the legend.

Table III. Description and statistical comparison of the snow survey depth datasets for new snow and peak snow accumulation.

		Year	New snow	Peak accumulation
Unburned	<i>n</i>	2012	66	159
	mean ± SD (cm)		15.0 ± 5.3	46.8 ± 16.5
Post-burn	<i>n</i>	2012	29	150
	mean ± SD (cm)		8.5 ± 5.0	54.3 ± 19.8
Unburned	<i>n</i>	2010	N/A	140
	mean ± SD (cm)		N/A	71.3 ± 17.9
Pre-burn	<i>n</i>	2010	N/A	88
	mean ± SD (cm)		N/A	71.9 ± 18.0
ANOVA	<i>F</i> -statistic	2012	16.47	0.02
	<i>p</i> -value		<0.001	0.88
ANOVA	<i>F</i> -statistic	2010	N/A	7.52
	<i>p</i> -value		N/A	0.007

The sample size (*n*) and mean and standard deviation are given for the sub-datasets from each field site and each year. The *F*-statistic and *p*-value are reported from ANOVA results testing the difference between the unburned and post-burn site in 2012 and unburned and pre-burn site in 2010.

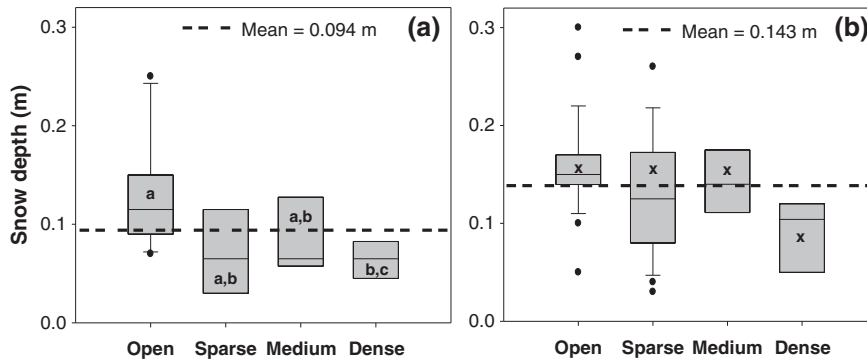


Figure 6. Box plots of new snow depth from 10/3 and 11/3 storms based on the four canopy categories from the 2012 unburned site (6a) and the 2012 post-burn site (6b). The mean of all data from each site is shown as a thick dotted line and differs significantly ($p < 0.01$) between the burned and unburned areas. The letters with the boxes refer to differences between the categories based on one-way ANOVA tests ($p < 0.05$).

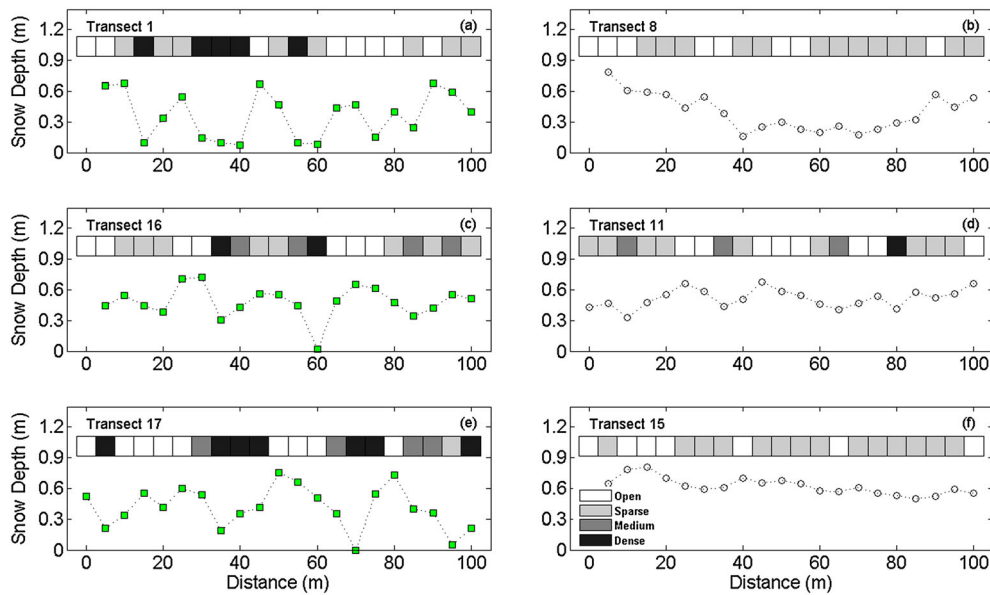


Figure 7. Observations of snow depths along six 100-m long transects in the 2012 unburned site (8a, 8c, 8e) and 2012 post-burn site (8b, 8d, 8f). The transect locations can be found using the transect number and Figure 2b and 2e. The vegetation density is shown as a shaded bar above the snow depth values.

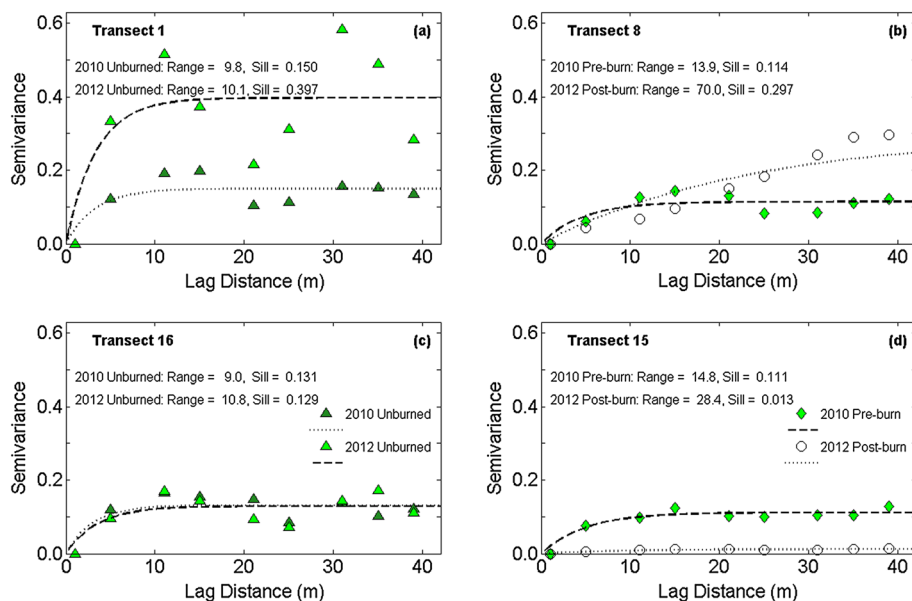


Figure 8. Semivariograms based on peak snow depth for four example transects from the 2012 unburned area (8a and 8c) and 2012 post-burn area (8b and 8d). The 2010 unburned and pre-burn semivariograms are also shown for the corresponding locations. The range and sill values from a best fit exponential relationship are shown. The transect locations can be found using the transect number and Figure 2b and 2e.

The post-burn area had a similar range of 7 to 97 cm depths (Figure 7) and a similar standard deviation of 17 cm, but different scales of spatial variability (Figure 7). The range of the semivariogram, or the length-scale for spatial variability, was 10 to 15 m in both areas in 2010 (both unburned and pre-burned) and in the unburned area in 2012. In contrast, the range increased to 30 to 70 m in the post-burn area and the sill (or magnitude of variability) decreased in most post-burn transects. Transect 15 showed a near doubling of the range (from 15 to 28 m) and an order of magnitude decrease in the sill (0.11 to 0.01 m^2), characteristic of the reduced spatial variability found across the post-burn area. However, both the range and sill increased following fire in transect 8 (Figure 8b), which was a steeper area with topographic convergence and changing east-west aspect (Figure 2e). The changes in post-fire semivariance at transect 8 were consistent with a shift from interception and canopy shading in a healthy forest to topographic shading and aspect controls after canopy loss.

In contrast to observations of greater new snow inputs in post-burned areas, the 2012 peak snowpack was larger in the unburned area compared with the post-burn area, despite observations of similar peak snow accumulation in these same areas prior to the fire in 2010. The peak snowpack depths before the fire, derived from 2010 LiDAR datasets, had similar mean values (Figure 9a) in the unburned and pre-burn areas (71 and 72 cm, respectively). Following the fire in 2012, the unburned and post-burn peak snowpack

depths were significantly different ($p = 0.007$), with means of 54 and 47 cm, respectively. The mean SWE: p ratio for all unburned forests was approximately 0.70 in 2010, decreasing to 0.63 in 2012 suggesting similar sublimation fluxes in both years, with lower SWE: p ratios driven by lower precipitation in 2012 (Figure 9b). In contrast to 2010, the SWE: p ratio for the post-burn area was significantly lower (SWE: $p = 0.53$) than all the healthy forest areas (Figure 9b) indicating higher winter sublimation fluxes following removal of canopy by fire.

In the unburned area, 2012 peak snowpack was significantly larger in open areas than sparse, medium or dense forest canopy ($p < 0.05$; Figure 10a) and had no relationship with topography ($p > 0.13$; Table IV). Canopy categories explained less variability in peak snowpacks in the post-burn area (Table III), differences only existed between two groups, open/sparse and medium/dense canopy categories (Figure 10b). In contrast to the unburned area, the peak snow accumulation in the post-burn area was linearly correlated ($p < 0.05$) with the aspect and elevation of the sampling locations (Table IV).

DISCUSSION

In this study, we quantified the impacts of high-severity fire on new snow accumulation and peak annual snowpacks using information from burned and unburned areas before and after canopy loss. We evaluated two sets of processes that have compensatory effects on net snow water inputs at peak snowpack in post-burned forests: (1) reduced interception by forest canopy results in greater new snow accumulation following fire and (2) increased winter season ablation of the snowpack following fire results in reduced peak snowpack volumes. The effects of interception on new snowfall and peak accumulation have been well-documented (Birkeland *et al.*, 1998; Hedstrom and Pomeroy 1998; Pomeroy *et al.*, 1998; Pomeroy *et al.*, 2002; Storck *et al.*, 2002; Veatch *et al.*, 2009; Varhola *et al.*, 2010), but winter season ablation, particularly because of sublimation, is difficult to measure and model (Molotch *et al.*, 2007; Gustafson *et al.*, 2010; Reba *et al.*, 2012). Using several lines of evidence, we demonstrated conclusively that vegetation exerts strong controls on the magnitude and distribution of snowpacks in healthy forests, and that canopy loss from fire can alter these snow-vegetation interactions and reduce the volume of snow water available to melt.

New snowfall during a single storm was strongly controlled by the vegetation density in healthy forests, consistent with numerous previous studies of interception under similar conditions. Locations in the unburned area categorized as open canopy had significantly larger new snow depths than areas categorized as dense canopy (averages of 11 and 7 cm, respectively), but no significant vegetation controls were observed in the post-burn area (Figure 6). The interception of new snowfall was estimated from a 15 cm storm on 9/3/2012 and 10/3/2012 using a nearby snow depth sensor at an open location (Figures 1

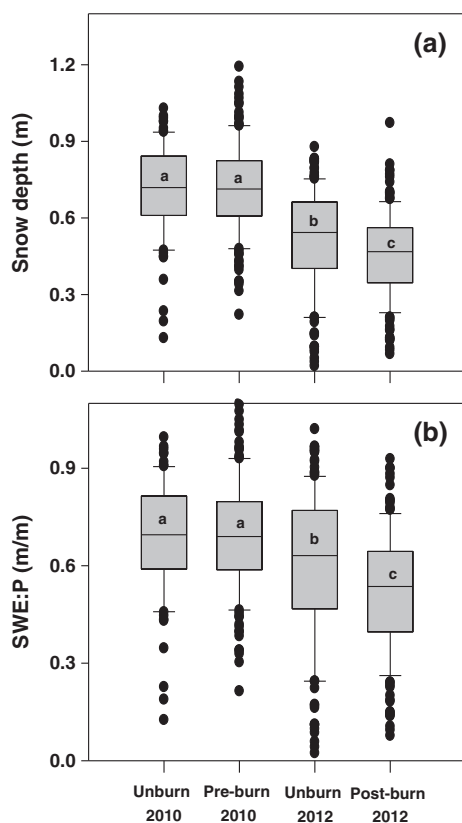


Figure 9. Box plots snow depth (9a) and snow water equivalent to winter precipitation ratio (SWE: p in 9b) at the peak snow accumulation in 2010 and 2012. The letters with the boxes refer to differences between the categories based on one-way ANOVA tests ($p < 0.05$).

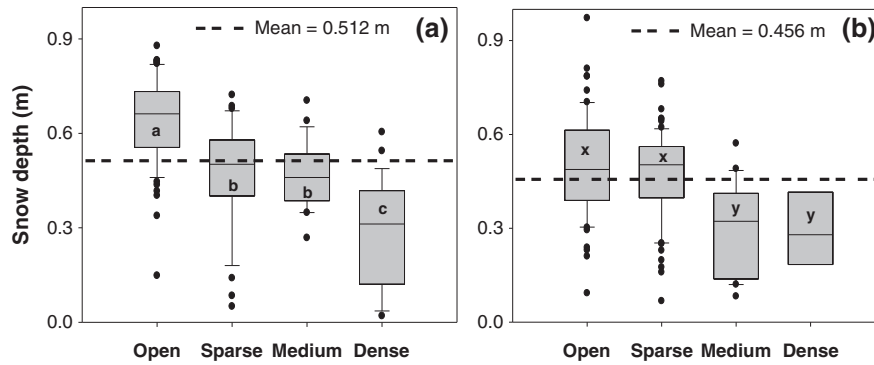


Figure 10. Box plots of snow depth at peak snow accumulation based on the four canopy categories from the 2012 unburned site (6a) and the 2012 post-burn site (6b). The mean of all data from each site is shown as a thick dotted line. The letters with the boxes refer to differences between the categories based on one-way ANOVA tests ($p < 0.05$).

and 2) but may have varied from 12 to 15 cm across the unburned area. These new snowfall measurements suggest that 25% to 45% of the new snow was intercepted in the unburned area, which is consistent with previous observations in similar conifer forests (Hedstrom and Pomeroy 1998; Pomeroy *et al.*, 1998; Varhola *et al.*, 2010). Although additional direct observations and modelling are needed to narrow the range of interception values for these forests, it is clear that reduced interception by forest canopy resulted in greater new snowfall inputs to the snowpack, which would portend higher peak snowpacks following fire.

In direct contrast to new snowfall, our results demonstrated that peak snowpacks were significantly smaller in the post-burn area compared with the unburned area (Figure 9 and Table III). Our observation of smaller peak snow accumulation following fire suggests that increased winter season ablation compensated for the reduced interception of new snowfall. The SWE: p ratios confirmed that substantial ablation occurred prior to peak snowpack in healthy forests during 2010 and 2012 (30% to 37% of the total winter precipitation), but significantly more ablation occurred in the post-burn area (47% of winter precipitation). The average air temperature was below 0°C until 1/3/2012, and the snowpack temperatures were below 0°C in all snow pits (Figure 5), which along with faceted

crystals throughout the pack, and were indication that melt was probably not a significant source of winter season ablation in 2012. The low wind speeds (Figure 3c) were not likely to cause significant scouring (Winstral and Marks 2002), making wind re-distribution an unlikely cause for the observed post-burn differences in peak snowpacks. This is further supported by semivariograms of snow depth that show scour and re-deposition is of limited importance in these systems (Figure 8). These observations of reduced winter season melt and wind scour suggest that the observed ablation of the snowpack was primarily due to sublimation, consistent with previous observations on nearby Redondo Mountain (Veatch *et al.*, 2009; Gustafson *et al.*, 2010)

Our results demonstrate a shift from vegetation to topographical controls in net snow accumulation following fire. The net result is an increase in winter sublimation losses in burn-affected areas even in these dominantly north-facing areas. Following the Las Conchas Fire, peak snowpack depths in the post-burn area had significant differences between open and dense canopy categories (Figure 10b), similar to the healthy forest; however, open canopy areas in the post-burn area had less snow than corresponding open areas in the unburned area (Figure 10a). The vegetation–snow interactions in healthy forests left a clear ‘signature’ on the spatial variability of peak snowpack depths, which showed a consistent increase in the spatial scale of variance at 10 to 15 m (Figure 8a, c). Following the fire, vegetation controls on peak snowpacks were reduced, and the spatial scale of variance increased to >30 m (Figure 8b, d). The change in the patterns of spatial variability in the post-burn area were consistent with the significant positive relationship between snowpack and aspect (northness) and suggests that topographic influences on winter season ablation become more important as vegetation influences decrease after the loss of the forest canopy.

A forest canopy alters both radiative and turbulent exchanges between the snow surface and the atmosphere, with dramatic effects on the snowpack energy balance and sublimation rates. Eddy-covariance measurements in the Reynolds Creek watershed in Idaho showed sublimation rates 3 to 10 times higher in open areas versus a forested

Table IV. Statistical results of linear regression and ANOVA tests for 2012 snow depth data (# and @ refer to linear regression and ANOVA tests, respectively) with respect to several independent variables.

	2012 unburn		2012 post-burn	
	r^2	p -value	r^2	p -value
Elevation#	0.02	0.82	0.16	0.041
Northness#	0.13	0.10	0.19	0.017
	2012 unburn		2012 post-burn	
	F -statistics	p -value	F -statistics	p -value
Aspect@	0.20	0.82	3.19	0.025
Canopy@	42.27	<0.001	11.24	<0.001

The correlation coefficient and p -value are reported from linear regressions performed on elevation and northness. The F -statistic and p -value were also reported from ANOVA tests on four aspect categories (north, south, east and west) and four canopy categories (open, sparse, medium and dense).

location (16% to 41% versus 5% to 8% of maximum SWE, respectively) (Reba *et al.*, 2012). In Reynolds Creek, the higher sublimation fluxes were attributed to increased turbulent transport of saturated air from the snowpack to the dry overlying atmosphere (Reba *et al.*, 2012), whereas studies in Colorado and New Mexico have suggested that higher sublimation fluxes are driven primarily from increased shortwave radiation inputs to the snowpack in open locations relative to canopy shaded locations (Rinehart *et al.*, 2008); Biederman *et al.*, in press). The different inferences drawn from these studies suggests that the relative importance of turbulent and radiative terms to snowpack sublimation fluxes varies on the basis of local climate, topographical and vegetation characteristics. Several studies from Redondo Mountain, less than 10 km away, have observed significant relationships between solar forcing and sublimation in canopy gaps with winter season sublimation losses from the snowpack of up to 40% (150–200 mm) in exposed locations (Musselman *et al.*, 2008; Veatch *et al.*, 2009; Gustafson *et al.*, 2010). The high snowpack sublimation rates on Redondo Mountain are by no means unique, and other observations in colder, more northern forests (Molotch *et al.*, 2007; Reba *et al.*, 2012) and treeless alpine areas (Cline 1997; Hood *et al.*, 1999; Knowles *et al.*, 2012) have found similar winter season vapour losses of up to 50% of total snowfall.

Our observations of a reduction in peak snowpacks following fire, combined with similar observations following insect-induced forest mortality (Biederman *et al.*, in press), highlight the need for new observations and mechanistic models that quantify both spatial and temporal variability in energy and water fluxes in topographically complex, snow-covered, forested terrain. Although such an accounting is beyond the datasets and scope of this paper, our results and other recent work do advance the conceptual understanding of how changes in snowpack energy balance affect peak snowpack volumes after fire. Canopy removal alters the local wind fields and turbulent transport, vapour pressure deficit, and longwave and shortwave radiation inputs in complex and coupled ways that are not well understood. At our field site, both observations and modelling suggest that shortwave radiation controls the spatial patterns of sublimation in nearby healthy forests (Rinehart *et al.*, 2008; Veatch *et al.*, 2009; Gustafson *et al.*, 2010) and thus likely also dominates the energy balance before snowmelt. The importance of shortwave radiation in the snowpack energy budget prior to melt is consistent with more detailed measurements of mountain snowpacks in California, Colorado and Canada (Cline 1997; Marks and Dozier 1998), Ellis *et al.*, 2011). The role of shortwave radiation is potentially enhanced at the study site by more cloudless days and nights, a high zenith and azimuth, and a very dry atmosphere. These inferences match the distributed modelling work of Rinehart *et al.*, (2008) who showed that scattering of shortwave radiation from adjacent snow-covered hillslopes could change the energy balance by $\pm 30 \text{ W/m}^2$ on Redondo Mountain or enough to sublimate up to 50% of the snowpack. We would expect shortwave radiation inputs to increase

after the loss of the forest canopy because of a decrease in canopy shading and increased scattering (because of increased albedo) from remote hillslopes during the day. Interestingly, the Rabbit Mountain site received an average daytime (7:00 to 19:00) radiation of 136 W/m^2 from 15/2/2012 to 15/3/2012, compared with 331 W/m^2 at the more south-facing Redondo meteorological station (Figures 1 and 3d), demonstrating the tremendous variability in radiation inputs. Longwave radiation inputs during the day are typically close to zero for cold, alpine (tree-less) snowpacks (Cline 1997; Marks and Dozier 1998), and a reduction in canopy volume from fire would decrease the emissivity of the canopy and generally reduce longwave energy inputs to the snowpack. During relatively cold and cloudless nights, we expect that the emission of longwave radiation increases and cools the surface of the snowpack following the removal of the forest canopy. We also expect the roughness length of the canopy to decrease following fire, which would increase turbulent exchange between the atmosphere and the snowpack. In these dry locations, the primary effect of increased turbulence would be to transport sublimated water vapour into the atmosphere.

Both longwave emission and increased transport of sublimated water to overlying atmosphere would serve to cool the snow surface effectively increasing the vapour pressure gradient within the snowpack. The crystal structure of the snowpacks reflected these stronger vapour pressure gradients across the snowpack in the post-burn area relative to the unburned area. The large faceted snow grains in the post-burn area (Figure 5b, d) are typical of shallow, porous snowpacks and larger temperature and vapour pressure gradients between the snow surface and ground (Dewalle and Rango 2008). Although faceted snow crystals also could result from near-surface processes of radiation recrystallization, melt-layer recrystallization and diurnal recrystallization (Birkeland 1998), warm daytime temperatures and increased solar inputs typically result in these features being short lived unless they are isolated from temperature and vapour pressure variability by large, new snow events. In contrast to a completely faceted snowpack resulting from strong vapour pressure gradients between the base of the snowpack and the atmosphere observed in the burned forest, unburned sites exhibited rounded crystals indicative of equilibrium metamorphism and weaker vapour pressure gradients. Presumably, both reduced turbulence (Reba *et al.*, 2012) and increased longwave inputs to the snowpack from overlying forests (Essery *et al.*, 2008; Pomeroy *et al.*, 2009) resulted in reduced vapour pressure gradients through the snowpack in the unburned forests. Although the snowpack structure records the differences in energy and mass fluxes between the two sites, the magnitude of different energy balance terms cannot be determined from our dataset, highlighting the need for improved observations and models of snowpack energy and mass balance following the loss of the forest canopy.

An improved understanding of how topography and vegetation interact to control spatial variability in the snowpack energy and mass balance is necessary to diagnose how the observed 10% reduction in the

peak snowpack following fire might scale to a larger area. Previous studies in nearby healthy forests found that snowpack sublimation was controlled by shortwave radiation (e.g. Musselman *et al.*, 2008; Veatch *et al.*, 2009); Gustafson *et al.*, 2011) indicating that sufficient diffusion and turbulent energy is present to transport water vapour into the atmosphere and that sublimation is likely 'energy limited' at this site. If a site were 'energy limited', increased energy inputs on a more south-facing, exposed hillslope would be expected to cause greater sublimation (e.g. Rinehart *et al.*, 2008) and melt (e.g. Ellis *et al.*, 2011). This is notable because our study area was largely north-facing, yet we observed that an additional 10% of the snowpack was lost as water vapour after the canopy was removed. A robust estimate of the impacts of increased winter season sublimation following fire on the larger-scale water balance will require combining a physically based model with a distributed measurement scheme to capture how vapour transport and energy budget terms co-vary in space and time across a mosaic of healthy forests and fire severity.

CONCLUSIONS

The increased winter season ablation following the Las Conchas Fire demonstrated the mitigating role that forest canopies play in reducing snowpack sublimation and potentially increasing the water available for vegetation and runoff. Our results suggest that in areas with high atmospheric water demand, such as the continental Rocky Mountains, canopy loss following forest disturbance could increase net winter season snow sublimation relative to a healthy forest. The increased winter season ablation reduced snow water inputs by 10% at a post-burn area as compared with a similar, nearby healthy forest, despite the observation that new snowfall increased following the loss of canopy. Snow-vegetation interactions that mitigate winter season snowpack sublimation in healthy forests shifted to topographical controls that can enhance sublimation in burn-affected areas. The relative importance of shortwave radiation to the snowpack energy balance and sublimation suggests that the 10% reductions in peak snow water storage found in these north-facing areas could be a conservative estimate for winter season ablation following fire. Further work is necessary to quantify interactions between topography and vegetation that alter winter season snow water partitioning following forest disturbance. Combined with faster melt following fire (Burles and Boon, 2011), changes in snow water partitioning prior to melt could have important ramifications for ecological health and downstream water resources.

ACKNOWLEDGEMENTS

This National Science Foundation (EAR 0910831, EAR 0724958) and Department of Energy (TES DE-SC0006968) supported this research. We would also like to acknowledge the Valles Caldera National Preserve and Bob Parmenter for access to the field site. Finally, we thank Jessica Lundquist for her outstanding comments that improved this paper.

REFERENCES

- Adams H, *et al.* 2011. Ecohydrological consequences of drought- and infestation-triggered tree die-off: insights and hypotheses. *Ecohydrology* **5**(2): 145–159. DOI: 10.1002/eco.233
- Anderson HW. 1956. Forest-cover effects on snow accumulation and melt in the Central Sierra Snow Laboratory. *American Geophysical Union Transactions* **37**: 307–312.
- Bales R, *et al.* 2006. Mountain hydrology of the western United States. *Water Resources Research* **42**: W08432.
- Barnett TP, Adam JC, Lettenmaier DP. 2005. Potential impacts of a warming climate on water availability in snow-dominated regions. *Nature* **438**: 303–309.
- Bethlahmy N. 1974. More streamflow after a bark-beetle epidemic. *Journal of Hydrology* **23**(3-4): 185–189.
- Bentz BJ, *et al.* 2010. Climate Change and Bark Beetles of the Western United States and Canada: Direct and Indirect Effects. *BioScience* **60**(8): 602–613. doi: <http://dx.doi.org/10.1525/bio.2010.60.8.6>
- Bergen JD. 1971. Vertical Profiles of Windspeed in a Pine Stand. *Forest Science* **17**(3): 314–321.
- Bernier PY. 1990. Wind-speed and snow evaporation in a stand of juvenile lodgepole pine in Alberta. *Canadian Journal of Forest Research-Revue Canadienne De Recherche Forestiere* **20**(3): 309–314. DOI: 10.1139/x90-045.
- Biederman JA, Brooks PD, Harpold AA, Gochis DJ, Gutmann E, Reed DE, Pendall E, Ewers BE. 2012. Multiscale observations of snow accumulation and peak snowpack following widespread, insect-induced lodgepole pine mortality. *Ecohydrology* DOI: 10.1002/eco.1342.
- Birkeland KW. 1998. Terminology and predominant processes associated with the formation of weak layers of near-surface faceted crystals in the mountain snowpack. *Arctic and Alpine Research* **30**(2): 193–199.
- Birkeland KW, Johnson RF, Schmidt DS. 1998. Near-surface faceted snow crystals formed by diurnal recrystallization: A case study of weak layer formation in the mountain snowpack and its contribution to snow avalanches. *Arctic and Alpine Research* **30**(2): 200–204.
- Breshears D, *et al.* 2005. Regional vegetation die-off in response to global-change-type drought. *Proceedings of the National Academy of Science* **102**(42): 15144–15148.
- Breshears DD, *et al.* 2009. Tree die-off in response to global change-type drought: mortality insights from a decade of plant water potential measurements. *Frontiers in Ecology and the Environment* **7**: 185–189. <http://dx.doi.org/10.1890/080016>
- Burles K, Boon S. 2011. Snowmelt energy balance in a burned forest plot, Crownsnest Pass, Alberta, Canada. *Hydrological Processes* **25**: 3012–3029. DOI: 10.1002/hyp.8067
- Campbell WG, Morris SE. 1988. Hydrologic response of the Pack River, Idaho, to the Sundance Fire. *Northwest Science* **62**: 165–170.
- Cline DW. 1997. Snow surface energy exchanges and snowmelt at a continental midlatitude Alpine site. *Water Resources Research* **33**: 689–701.
- Dewalle DR, Rango A. 2008. *Principles of Snow Hydrology*. Cambridge University Press: New York.
- Ellis CR, Pomeroy JW, Essery RLH, Link TE. 2011. Effects of needleleaf forest cover on radiation and snowmelt dynamics in the Canadian Rocky Mountains. *Can. J. For. Res.* **41**: 608–620.
- Elder K, Rosenthal W, Davis RE. 1998. Estimating the spatial distribution of snow water equivalence in a montane watershed. *Hydrological Processes* **12**(10-11): 1099–1808. doi: 10.1002/(sici)1099-1085(199808/09)12:10/11<1793::aid-hyp695>3.3.co;2-b
- Essery R, Pomeroy J, Ellis C, Link T. 2008. Modeling longwave radiation to the snow below forest canopies using hemispherical photography or linear regression. *Hydrological Processes* **22**(15): 2788–2800.
- Gustafson JR, Brooks PD, Molotch NP, Veatch WC. 2010. Estimating snow sublimation using natural chemical and isotopic tracers across a gradient of solar radiation. *Water Resources Research* **46**. DOI: 10.1029/2009WR009060
- Haupt HF. 1951. Snow accumulation and retention on ponderosa pine lands in Idaho. *Journal of Forestry* **49**: 869–871.
- Hedstrom NR, Pomeroy JW. 1998. Measurements and modelling of snow interception in the boreal forest. *Hydrological Processes* **12**(10-11): 1611–1625.
- Hood E, Williams M, Cline D. 1999. Sublimation from a seasonal snowpack at a continental mid-latitude alpine site. *Hydrological Processes* **13**: 1781–1797.
- Jost G, Weiler M, Gluns DR, Alila Y. 2007. The influence of forest and topography on snow accumulation and melt at the watershed-scale. *Journal of Hydrology* **347**(1-2): 101–115. doi: 10.1016/j.jhydrot.2007.09.006.

- Kittredge J. 1953. Influences on snow in the ponderosa-sugar pin-fir zone of the central Sierra Nevada. *Hilgardia* **22**: 1–99.
- Knowles JF, Blaken PD, Williams MW, Chowanski KM. 2012. Energy and surface moisture seasonally limit evaporation and sublimation from snow-free alpine tundra. *Agricultural and Forest Meteorology* **157**: 106–115.
- Lawler RR, Link TE. 2011. Quantification of incoming all-wave radiation in discontinuous forest canopies with application to snowmelt prediction. *Hydrological Processes* **25**: Doi:10.1002/hyp.8150.
- Liu F, Bales RC, Conklin MH, Conrad ME. 2008. Streamflow generation from snowmelt in semi-arid, seasonally snow-covered, forested catchments, Valles Caldera, New Mexico. *Water Resources Research* **44**(12): W12443. doi: 10.1029/2007WR006728.
- Mahat V, Tarboton DG. 2012. Canopy radiation transmission for an energy balance snowmelt model. *Water Resources Research* **48**: W01534. doi:10.1029/2011WR010438
- Marks D, Dozier J. 1998. Climate and energy exchange at the snow surface in the Alpine Region of the Sierra Nevada: 2. Snow cover energy balance. *Water Resources Research* **28**: 3043–3054.
- Marlon JR, *et al.* 2012. Long-term perspective on wildfires in the western USA. *Proceedings of the National Academy of Science* **109**(9): E535–E543.
- Miller J, Safford H, Crimmins M, Thode A. 2009. Quantitative evidence for increasing forest fire severity in the Sierra Nevada and Southern Cascade Mountains, California and Nevada, USA. *Ecosystems* **12**: 16–32.
- Molotch NP, *et al.* 2007. Estimating sublimation of intercepted and sub-canopy snow using eddy covariance systems. *Hydrological Processes* **21**(12): 1567–1575. DOI: 10.1002/hyp.6719.
- Molotch NP, Brooks PD, Burns SP, Litvak M, Monson RK, McConnell JR, Musselman K. 2009. Ecohydrological controls on snowmelt partitioning in mixed-conifer sub-alpine forests. *Ecohydrology* **2**(2): 129–142. DOI: 10.1002/eco.48
- Molotch NP, Blanken PD, Link TE. 2011. Snow: Hydrological and Ecological Feedback in Forests. In *Forest Hydrology and Biogeochemistry: Synthesis of Past Research and Future Directions*. eds. Levin DF, *et al.* Ecological Studies **216**(5): 541–555.
- Musselman K, Molotch NP, Brooks PD. 2008. Effects of vegetation on snow accumulation and ablation in a mid-latitude sub-alpine forest. *Hydrological Processes* **22**(15): 2767–2776. doi:10.1002/hyp.7050
- NCALM National Center for Airborne Mapping. 2010. Critical Zone Observer LiDAR http://opentopo.sdsc.edu/metadata/2010_NCALM_CZO_Project_Report_Jemez.pdf. Accessed: 11/15/2012.
- NOAA. 2012. <http://www.ncdc.noaa.gov/sotc/fire/>. Accessed: 7/11/2012.
- Pomeroy JW, Parviainen J, Hedstrom N, Gray DM. 1998. Coupled modeling of forest snow interception and sublimation. *Hydrological Processes* **12**(15): 2317–2337.
- Pomeroy JW, Gray DM, Hedstrom NR, Janowicz JR. 2002. Prediction of seasonal snow accumulation in cold climate forests. *Hydrological Processes* **16**(18): 3543–3558.
- Pomeroy JW, Marks D, Link T, Ellis C, Hardy J, Rowlands A, Granger R. 2009. The impact of coniferous forest temperature on incoming longwave radiation to melting snow. *Hydrological Processes* **23**: 2513–2525.
- Pomeroy JW, Fang X, Ellis C. 2012. Sensitivity of snowmelt hydrology in Marmot Creek, Alberta, to forest cover disturbance. *Water Resources Research* **48**(12): 1891–1904.
- Potts DF. 1984. Hydrologic impacts of a large-scale mountain pine beetle (*Dendroctonus Ponderosae* Hopkins) epidemic. *Water Resources Bulletin*, **20**(3): 373–377.
- Pugh ET, Gordon ES. 2012. A conceptual model of water yield effects from beetle-induced tree death in snow-dominated lodgepole pine forests. *Hydrological Processes*. DOI: 10.1002/hyp.9312
- Pugh ET, Small EE. 2011. The impact of pine beetle infestation on snow accumulation and melt in the headwaters of the Colorado River. *Ecohydrology*. DOI: 10.1002/eco.239
- Raffa KF, *et al.* 2008. Disturbances prone to anthropogenic amplification: the dynamics of bark beetle eruptions. *BioScience* **58**(6): 501–517.
- Reba, ML, J Pomeroy, D Marks, TE Link. 2012. Estimating surface sublimation losses from snowpacks in a mountain catchment using eddy covariance method and turbulent transfer calculations. *Hydrological Processes*. DOI: 10.1002/hyp.8372.
- Rinehart AJ, Vivoni ER, Brooks PD. 2008. Effects of vegetation, albedo, and solar radiation sheltering on the distribution of snow in the Valles Caldera, New Mexico. *Ecohydrology*, **1**(3): 253–270. DOI: 10.1002/eco.26
- Seibert J, McDonnell JJ, Woodsmith RD. 2010. Effects of wildfire on catchment runoff response: a modelling approach to detect changes in snow-dominated forested catchments. *Hydrology Research* **41**(5): 378–390.
- Serreze MC, Clark MP, Armstrong RL, McGinnis DA, Pulwarty RS. 1999. Characteristics of western United States snowpack from telemetry (SNOTEL) data. *Water Resour. Res.* **35**: 2145–2160.
- Storck P, Lettenmaier DP, Bolton SM. 2002. Measurement of interception and canopy effects on snow accumulation and melt in a mountainous maritime climate, Oregon, United States.
- Sheskin D. 2004. *Handbook of parametric and non-parametric procedures*. Chapman and Hall: Boca Raton, FL.
- Troendle CA, King RM. 1987. The effect of partial and clearcutting on streamflow at Deadhorse Creek, Colorado. *Journal of Hydrology* **90**(1–2): 145–157. DOI: 10.1016/0022-1694(87)90177-6.
- Varhola A, Coops NC, Weiler M, Moore RD. 2010. Forest canopy effects on snow accumulation and ablation: An integrative review of empirical results. *Journal of Hydrology* **392**: 219–233.
- Veatch W, Brooks PD, Gustafson JR, Molotch NP. 2009. Quantifying the effects of forest canopy cover on net snow accumulation at a continental, mid-latitude site. *Ecohydrology* **2**(2): 115–128. DOI: 10.1002/eco.45
- Westerling AL, Hidalgo HG, Cayan DR, Swetnam TW. 2006. Warming and earlier spring increase western US forest wildfire activity. *Science* **313**: 940–943.
- Western Regional Climate Center (WRCC). <http://www.wrcc.dri.edu/cgi-bin/cliMAIN.pl?nmlosa>. Accessed: 7/11/2012.
- Winkler R, Boon S, Zimonick B, Baleshta K. 2010. Assessing the effects of post-pine beetle litter on snow albedo. *Hydrological Processes* **24**(6): 803–812.
- Winstral A, Marks D. 2002. Simulating wind fields and snow redistribution using terrain-based parameters to model snow accumulation and melt over a semi-arid mountain catchment. *Hydrological Processes* **16**(18): 3585–3603.
- Zhang M, Wei X. 2012. The cumulative effects of forest disturbance on streamflow in a large watershed in the central interior of British Columbia Canada. *Hydrol. Earth Syst. Sci. Discuss* **9**: 2855–2895.